NiTi and NiTi-TiC Composites: Part III. Shape-Memory Recovery

K.L. FUKAMI-USHIRO and D.C. DUNAND

The transformation behavior of near-equiatomic NiTi containing 0, 10, and 20 vol pct TiC particulates is investigated by dilatometry. Undeformed composites exhibit a macroscopic transformation strain larger than predicted when assuming that the elastic transformation mismatch between the matrix and the particulates is unrelaxed, indicating that the mismatch is partially accommodated by matrix twinning during transformation. The thermal recovery behavior of unreinforced NiTi which was deformed primarily by twinning in the martensite phase shows that plastic deformation by slip increases with increasing prestrain, leading to (1) a decrease of the shape-memory strain on heating, (2) an increase of the two-way shape-memory strain on cooling, (3) a widening of the temperature interval over which the strain recovery occurs on heating, and (4) an increase of the transformation temperature hysteresis. For NiTi composites, the recovery behavior indicates that most of the mismatch during mechanical deformation between the TiC particulates and the NiTi matrix is relaxed by matrix twinning. However, some relaxation takes place by matrix slip, resulting in the following trends with increasing TiC content at constant prestrain: (1) decrease of the shape-memory strain on heating, (2) enhancement of the two-way shape-memory strain on cooling, and (3) broadening of the transformation interval on heating.

I. INTRODUCTION

As reviewed recently by, *e.g.*, References 1 through 11, the shape-memory behavior exhibited by many allotropic, ordered alloys is the result of the thermoelastic nature of their phase transformation. In near-equiatomic NiTi alloys, the low-temperature B19' phase (martensite M) consists of equal fractions of 24 variants with different crystallographic orientations. The B19' structure deforms by twinning up to tensile strains of about 8 pct, resulting in a strong texture, as the optimally oriented variants grow at the expense of the less-favorably oriented variants. Upon heating above the A_f temperature and complete allotropic transformation of the twinned B19' phase (martensite M') to the untwinned high-temperature B2 phase (austenite β), the strain accumulated by twinning of the martensite is recovered. If, upon subsequent cooling, the original martensite M with equal volume fractions of the 24 possible variants is formed, the recovered strain is retained. This shape-memory effect (SME) can be repeated if the martensitic sample is again mechanically deformed. However, if, upon cooling, the martensite M' with oriented variants is formed so as to relax internal elastic stresses, the transformation is biased, some of the strain recovered upon heating is lost, and the sample adopts a shape intermediate between those of the deformed and undeformed states. This so-called two-way shape-memory effect (TWSME) can be repeated upon further thermal cycling between the austenite and martensite temperature ranges of the matrix. Both memory effects, SME and TWSME, have been exploited in applications such as actuators, connectors, heat engines, control systems, active dampers, self-erectable structures, and medical devices.[4,12–18]

The TWSME relies on biasing the formation of martensite by elastic stresses, which can originate from external or internal sources. For example, an elastic spring or a weight attached to a NiTi element can provide an external biasing force, resulting in a device with TWSME functionality.[16,17,18] The external bias can also originate from an elastic layer applied as a coating on the surface of the NiTi element. Hornbogen and co-workers[19,20] reported enhanced SME and TWSME for silicone-coated NiTi strips and springs. Finally, the biasing stresses can be internal, for instance, produced by stiff particles[21] or dislocations.[4] In the latter case, mechanical training for the TWSME involves slip deformation of the martensite and arrangement of the dislocations such that they are in equilibrium with the deformed martensitic structure. The stress field of these dislocations, which remain in the austenite phase after the phase transformation, biases the formation of the martensite upon cooling, resulting in the same equilibrium configuration of martensite variants as before the thermal excursion.

The present article is the third in a series investigating the thermal and mechanical behavior of titanium-rich NiTi composites containing TiC particulates. In a first article,[22] we investigated by calorimetry the phase transformation behavior of the undeformed composites as a function of the number of thermal cycles around the allotropic temperature. In a second article,[23] we examined the compressive mechanical behavior of these NiTi-base composites. Deformations to large strains for composites with a martensitic matrix (at low temperature) or an austenitic matrix (at high temperature) were investigated to study the effect of mismatch between the elastic TiC reinforcement and the NiTi matrix deforming by twinning (below the allotropic temperature) or stress-induced transformation (above the allotropic temperature). A companion article[24] reports on

K.L. FUKAMI-USHIRO, formerly Graduate Student, Department of Materials Science and Engineering, Massachusetts Institute of Technology, is Development Engineer with Raychem Corp., Menlo Park, CA 94025. D.C. DUNAND, AMAX Assistant Professor, is with the Department of Materials Science and Engineering, Massachusetts Institute of Technology, Cambridge, MA 02139.

Manuscript submitted March 14, 1995.

Table I. Linear Coefficients of Thermal Expansion α (10^{-6} K^{-1}) As Measured on Annealed, Undeformed Specimens and As Predicted by Equation [5]

		NiTi	NiTi-10TiC	NiTi-20TiC
Martensite	measured			
	heating	8.1	7.6	8.3
	cooling	8.9	8.3	8.2
	average	8.5	8.0	8.3
	predicted	8.5*	8.3	8.1
Austenite	measured			
	heating	12.6	12.0	11.7
	cooling	11.5	11.6	11.0
	average	12.1	11.8	11.4
	predicted	12.1*	11.5	10.9

*Assumed equal to the measured value.

neutron diffraction measurements of internal stresses and crystallographic orientation during deformation and after shape-memory recovery of these materials. In the present article, we examine the shape-memory recovery of martensitic NiTi and NiTi-TiC composites deformed at room temperature as functions of TiC volume fraction and mechanical prestrain. The SME and TWSME are discussed in light of the mismatch created by the inert TiC particles in the matrix, which, as explained previously, are expected to increase the elastic stresses stored in the composite.

II. EXPERIMENTAL PROCEDURES

Specimens were fabricated by vacuum hot pressing, followed by hot-isostatic pressing of prealloyed NiTi powders (99.9 pct pure, 70-μm average size, from Special Metals Corp., New Hartford, NY) and TiC particles (99.5 pct pure, with size between 44 and 100 μm, from Cerac, Inc., Milwaukee, WI), as described in more detail elsewhere.[23,25] The densified specimens of unreinforced NiTi, NiTi with 10 vol pct TiC, and NiTi with 20 vol pct TiC (labeled in what follows as NiTi, NiTi-10TiC, and NiTi-20TiC, respectively) were cut by electrodischarge machining into 5 $\times$ 5 $\times$ 10 mm right-parallelepiped samples, with tolerances within 5 μm of the nominal dimensions and within 0.25 deg of orthogonality. These samples were annealed in a titanium-gettered, 99.9 pct argon atmosphere at 930 °C for 1 hour, furnace-cooled to 400 °C at an average rate of 4.5 K·min^{-1}, and air-cooled to room temperature at a rate of about 20 K·min^{-1}. The samples were then deformed in uniaxial compression at room temperature to maximum strain values of 2, 3, 6, and 9 pct, as described in more detail elsewhere.[23,25]

Specimen strain after mechanical testing, determined from the average of multiple point-micrometer measurements of the sample length, was systematically less (by up to 0.5 pct) than the strain measured by the linear voltage displacement transducer (LVDT) during mechanical testing. This discrepancy could be due to mechanical strain recovery upon unloading at low stress values, for which the LVDT measurement is imprecise, or initial thermal recovery during specimen handling, as heat transferred from fingertips may have induced partial transformation. Dilatometry results presented in the present article indeed show that initiation of thermal recovery may occur at body temperature. In the following, we base our measurements on the sample strain measured by point micrometer just before the thermal recovery.

Each specimen was thermally recovered in a dilatometer (from E. Orton Jr. Ceramic Foundation, Westerville, OH) outfitted with a quartz sample holder and a quartz push-rod, which exerted a constant negligible compressive stress of 39 kPa on the specimen. The samples were heated in air from 20 °C to a maximum temperature of at least 275 °C at a rate of 1 K·min^{-1}, followed by cooling to 20 °C at the same rate. During this temperature cycle, the sample length was measured by an LVDT at the cold end of the push-rod, and the sample temperature was monitored by a thermocouple glued to the sample, with an absolute accuracy of 1.5 K. Experimental data were corrected for the thermal expansion of the quartz holder ($5 \cdot 10^{-7}$ K^{-1}[26]). Because the maximum temperature at the end of heating varied between 275 °C and 325 °C from specimen to specimen, the data above 275 °C were not reported. The cooling curves were shifted along the length axis such that the sample lengths were equal at 275 °C on heating and cooling.

The accuracy of the system was tested with a 6061-T6 aluminum sample, the coefficient of thermal expansion of which was measured as $25.4 \cdot 10^{-6}$ K^{-1} between 20 °C and 300 °C, in good agreement with a literature value of $25.5 \cdot 10^{-6}$ K^{-1} for 99.6 pct pure aluminum (Al-1060) measured in the same temperature range.[27]

III. RESULTS

As reported earlier,[23,25] the TiC particles are well distributed within the matrix and the particle-matrix interface is unreacted and pore-free. Densities of NiTi, NiTi-10TiC, and NiTi-20TiC are, respectively, 99.4, 98.8, and 90.6 pct of the theoretical rule-of-mixture values because of residual porosity in matrix and reinforcement.[23] In the following, we assume that the porosity has no effect on the shape-memory recovery of the samples, as discussed in more detail in companion articles.[22,23,24]

A. *Undeformed Specimens*

Dilatometry experiments were first performed on annealed, undeformed samples to characterize both the coefficient of thermal expansion and the transformation expansion of the untwinned matrix. Coefficients of thermal expansion for the samples in their fully martensitic and fully austenitic phases were determined in the temperature regions straddling transformation. As listed in Table I, the coefficients of thermal expansion decrease with increasing TiC content.

The phase transformation resulted in sharp departures from the linear thermal expansion slopes. As shown in Figure 1 and as listed in Table II, the linear allotropic expansion $\Delta L/L$ for the transformation decreases with increasing TiC content. Furthermore, the transformation temperatures are shifted to lower temperatures and the temperature interval over which the transformation takes place broadens.

B. *Deformed Specimens*

Figure 2 shows the stress-strain curves of NiTi and NiTi-TiC specimens for the largest maximum strain, e_{max} = 9

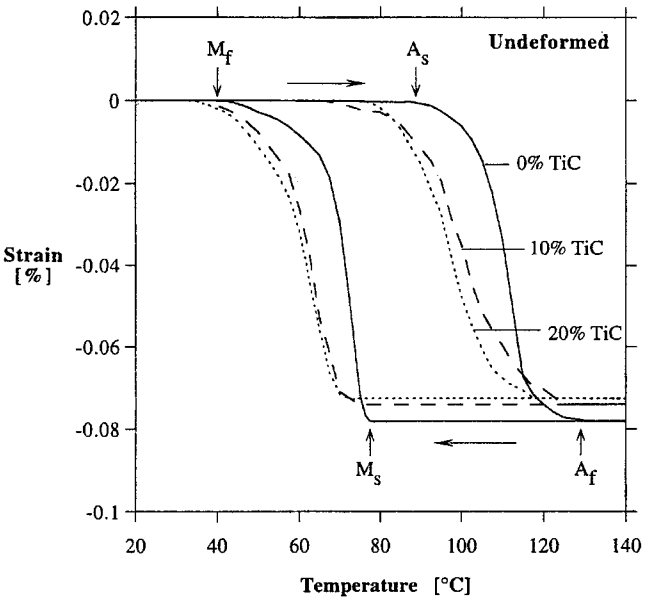

Fig. 1—Transformation strain upon heating and cooling for undeformed specimens.

Table II. Linear Allotropic Expansion $\Delta L/L$ (10^{-4}) upon Phase Transformation, As Measured on Annealed, Undeformed Specimens and As Predicted by Equation [7]

	NiTi	NiTi-10TiC	NiTi-20TiC
Measured	7.81	7.40	7.25
Predicted	7.81*	6.86	5.95

*Assumed equal to the measured value.

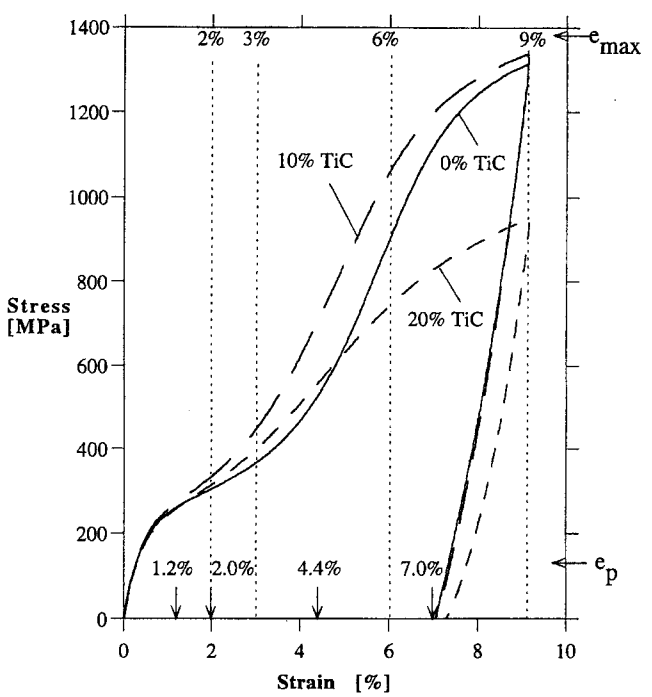

Fig. 2—Compressive stress-strain curves for the largest maximum strain e_{max} = 9 pct. Values for the other maximum strain e_{max} (for which unloading starts) are indicated with dotted lines, and values for the corresponding prestrain e_p (for which unloading is completed) are marked with arrows.

pct. The stress is corrected for porosity by multiplying the macroscopic sample cross-sectional area by their normalized density, and the plots show both compressive stress and compressive strain as positive values, a convention followed throughout this article. Specimens deformed to lower maximum strains (e_{max} = 2, 3, and 6 pct) exhibited stress-strain curves which overlapped with the curves shown in Figure 2 to within a stress of about 30 MPa. The plastic strain upon full unloading, referred to in the following as prestrain e_p, is also indicated in Figure 2. The stress-strain curves in Figure 2 are in good agreement with those reported in an earlier article,[23] except for the curve of NiTi-20TiC which shows lower stresses than the corresponding stress-strain curve in our earlier article[23] at strains above 3 pct. Because the specimen length in the present study is smaller than in the previous study,[23] the discrepancy may be due to errors induced by end effects. Because the stress state at the end of compression specimens is not uniaxial as a result of friction with the platens,[28] and because NiTi strain response is sensitive to stress triaxiality,[29] the strain near the sample ends was probably different from that in the middle of the sample, where the stress is uniaxial.

In dilatometric recovery experiments conducted on deformed specimens, the sample thermal expansion was eliminated by defining the recovery R on heating as

$$R = \frac{L(T) - L_M(T)}{L_A(T) - L_M(T)} \quad [1]$$

where $L(T)$ is the measured length of the specimen at the temperature T, $L_A(T)$ is the length of the fully recovered austenitic sample, and $L_M(T)$ is the hypothetical length of the deformed, unrecovered martensitic sample:

$$L_A(T) = L_0(1 + \alpha_A \Delta T) \quad [2]$$

$$L_M(T) = L_0'(1 + \alpha_M \Delta T) \quad [3]$$

where α is the coefficient of thermal expansion, $\Delta T = T - T_0$ is the temperature excursion above room temperature T_0, L_0 is the length of the undeformed sample at T_0, and $L_0' = L_0(1 - \varepsilon_p)$ is the length of the deformed sample at T_0 after mechanical testing. In the definition of the length L_A (Eq. [2]), the strain associated with the phase transformation $\Delta L/L = 7.2 \cdot 10^{-4}$ to $7.8 \cdot 10^{-4}$ is neglected, because it is much smaller than the mechanical prestrain $e_p = 2 \cdot 10^{-2}$ to $9 \cdot 10^{-2}$. While the recovery R is used to compare the recovery capabilities of specimens with different prestrains e_p and thus different degrees of recoverable strains, the recovery strain e, defined as

$$e = \frac{L(T) - L_M(T)}{L_0} \quad [4]$$

is directly comparable to the mechanical prestrain e_p.

Figure 3 shows a typical dilatometry curve for a full temperature cycle, where the specimen strain e or recovery R is plotted as a function of temperature. The dilatometry curve can be separated in regions with different slopes. During initial heating of the deformed martensite M' in region 1, some strain is recovered. The main recovery by the ($M' \rightarrow \beta$) transformation is characterized by a large expansion in region 2 between A_s and A_f, while post-transformation recovery takes place in region 3, where most of the matrix consists of austenite. Upon cooling from the maxi-

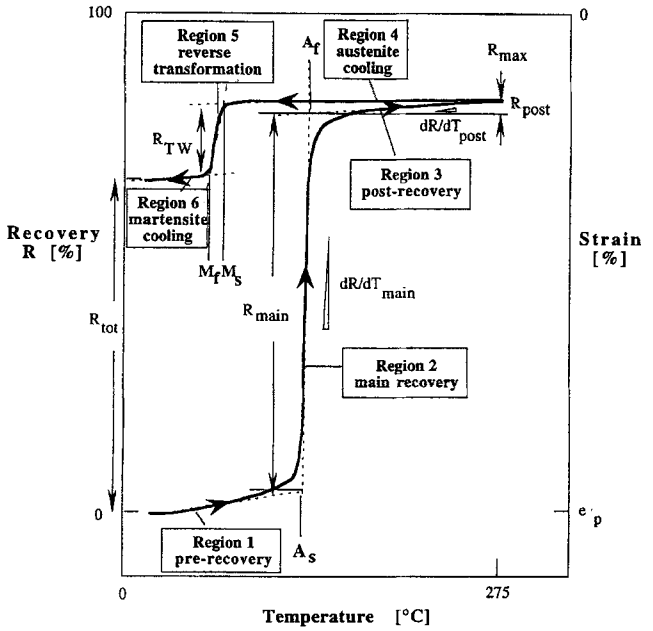

Fig. 3—Schematic dilatometry curve (heating and cooling) showing the six main regions, the transformation temperatures, and the different parameters used in the text.

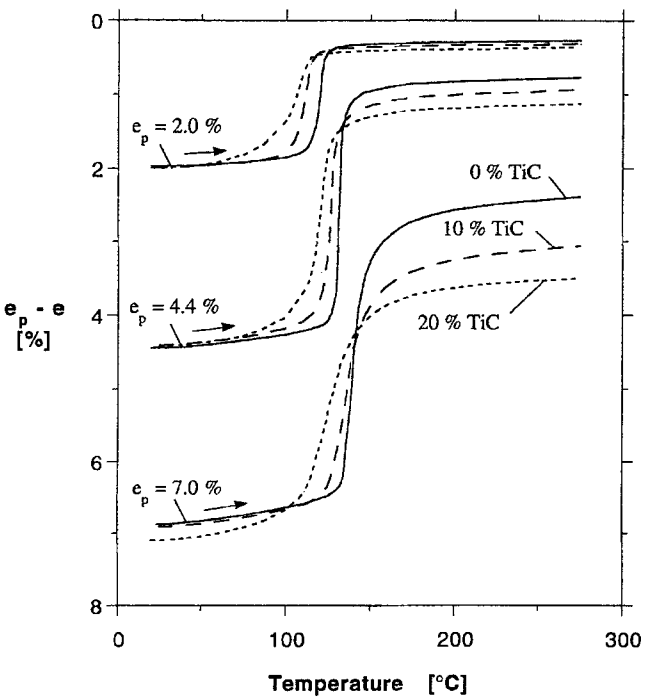

Fig. 4—Strain $e_p - e$ upon heating of specimens deformed to prestrains e_p = 2.0, 4.4, and 7.0 pct.

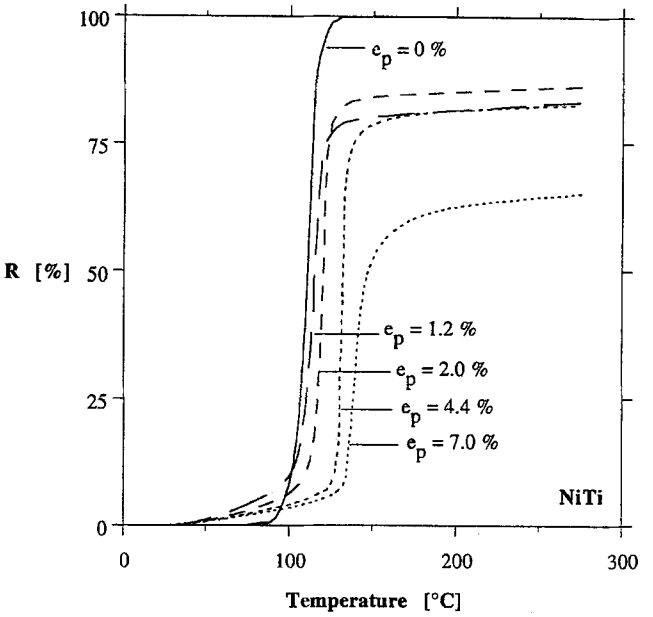

Fig. 5—Extent of recovery R upon heating for NiTi deformed to different prestrains e_p.

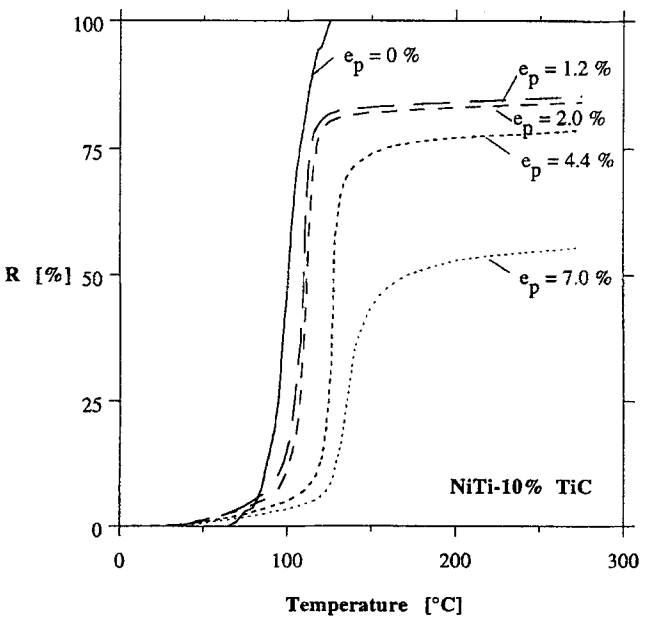

Fig. 6—Extent of recovery R upon heating for NiTi-10TiC deformed to different prestrains e_p.

mum temperature, negligible recovery is measured in region 4, confirming that the small recovery measured upon heating in the corresponding region 3 is not an experimental artifact. In region 5 between M_s and M_f, the austenite β transforms back to martensite. However, prior deformation may prevent the martensite from recovering its fully annealed, random grain structure. The martensitic structure obtained after the first thermal recovery cycle is referred to as M'', which is associated with a net contraction or expansion in region 5, depending on the magnitude of the prestrain. Finally, in region 6, the martensite M'' is cooled to room temperature. As the transformation temperatures are defined as the intersection of the slopes of adjacent regions, they are not directly comparable to values determined by calorimetry in companion articles.[22,23,25]

Figure 4 shows the strain $e_p - e$ as a function of temperature upon heating for all samples deformed to three different mechanical prestrains: $e_p = 2 \pm 0.05$ pct (e_{max} = 3 pct, at the end of the twinning region of the stress-strain curve, Figure 2), $e_p = 4.4 \pm 0.2$ pct (e_{max} = 6 pct, in the transition region), and $e_p = 7 \pm 0.1$ pct (e_{max} = 9 pct, in the plastic slip region). The recovery R as a function of temperature upon heating for theses samples is shown in Figures 5 through 7. The following are apparent from Fig-

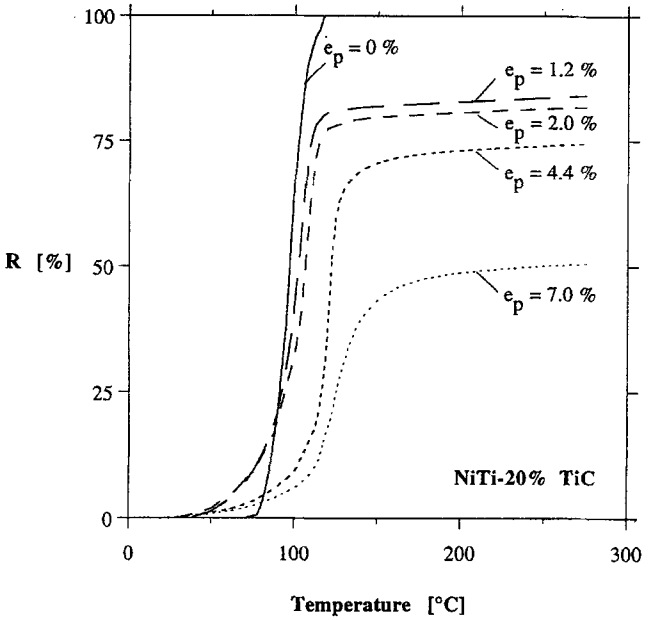

Fig. 7—Extent of recovery R upon heating for NiTi-20TiC deformed to different prestrains e_p.

ures 4 through 7: (1) with increasing prestrain, the transformation temperatures A_s and A_f increase (Figures 8(a) and (b)), recovery strain e increases, and recovery extent R decreases; and (2) with increasing TiC volume fraction, recovery strain e and recovery extent R decrease, transformation temperatures A_s and A_f decrease, and the transformation temperature range A_f to A_s increases (Figures 8(a) and (b)).

To facilitate comparison of the recovery behavior upon cooling in region 5, recovery strains e are adjusted in Figures 9 through 11 to emanate from a value of 0 pct at a temperature of 100 °C. In Figure 9, the cooling behavior of NiTi is shown as a function of prestrain. At prestrains below 2 pct, the ($\beta \rightarrow M'$) expansion in region 5 (shown in Figure 1 for e_p = 0 pct) decreases with increasing prestrain and becomes a contraction for prestrains larger than 2 pct, indicating that the TWSME increases with prestrain. Figures 10 and 11 show the cooling behavior for different levels of prestrain for NiTi-10TiC and NiTi-20TiC, respectively. Compared to unreinforced NiTi, the composites exhibit lower transformation temperatures M_s and M_f, a wider transformation temperature range M_s to M_f (Figures 12(a) and (b)), and, except for the prestrain of e_p = 4.4 pct, a smaller total strain recovery and larger TWSME contraction.

IV. DISCUSSION

A. *Undeformed Specimens*

Residual internal stresses, created during cooling from annealing temperature by the thermal and transformation expansion mismatches between matrix and reinforcement, may influence the subsequent thermoelastic transformation and thus the deformation behavior of the specimens. However, these elastic stresses are small and isotropic, as calculated in an earlier article[22] and as verified by neutron diffraction experiments in a companion article.[24] Furthermore, as discussed later, accommodation by twinning of the matrix can further relax mismatch stresses. Therefore, we assume in the present study that differences in recovery behavior observed between specimens with different TiC volume fractions are not due to different levels of elastic residual stresses before deformation but rather to differences in deformation behavior.

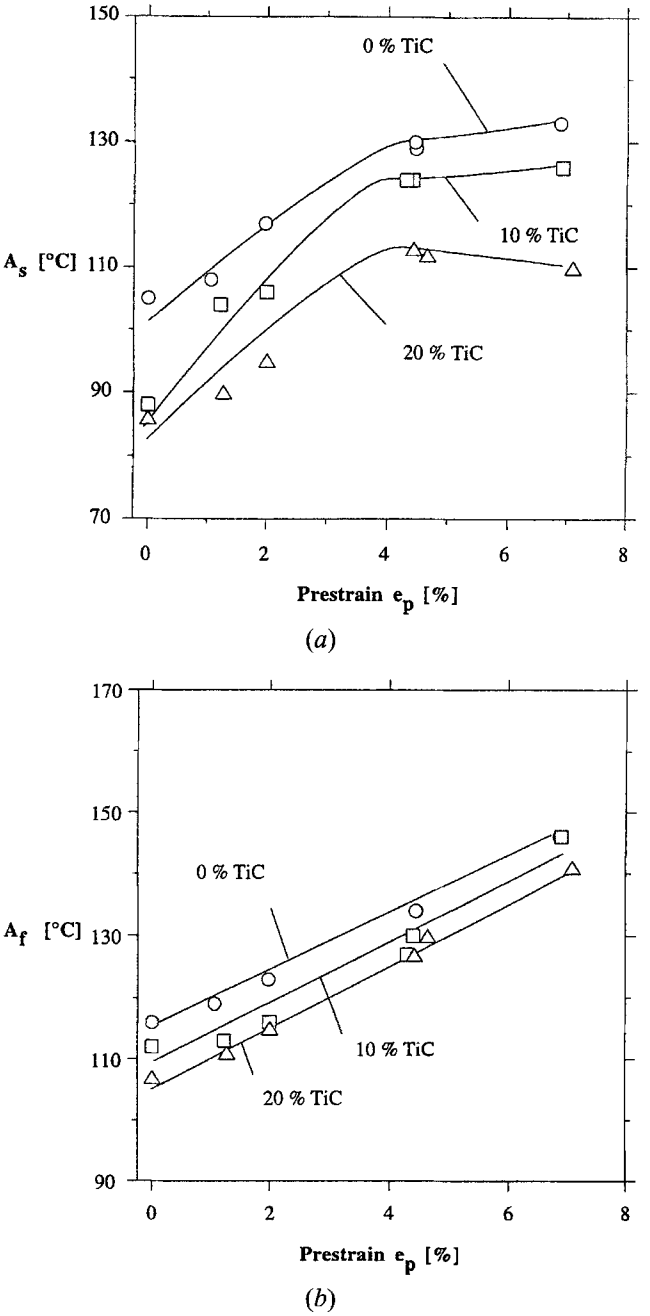

Fig. 8—(*a*) Austenite start temperature A_s and (*b*) Austenite finish temperature A_f (measured by dilatometry) as a function of prestrain e_p.

1. *NiTi*

Coefficients of thermal expansions are measured as $\alpha_M = 8.5 \cdot 10^{-6}\ K^{-1}$ for martensitic NiTi and $\alpha_A = 12.1 \cdot 10^{-6}\ K^{-1}$ for austenitic NiTi (Table I). These values are in reasonable agreement with those reported in References 2 and 13 ($\alpha_M = 6.6 \cdot 10^{-6}\ K^{-1}$ and $\alpha_A = 11 \cdot 10^{-6}\ K^{-1}$) but less so with values calculated from density measurements by Hsu *et al.*[30] ($\alpha_A = 15 \cdot 10^{-6}\ K^{-1}$).

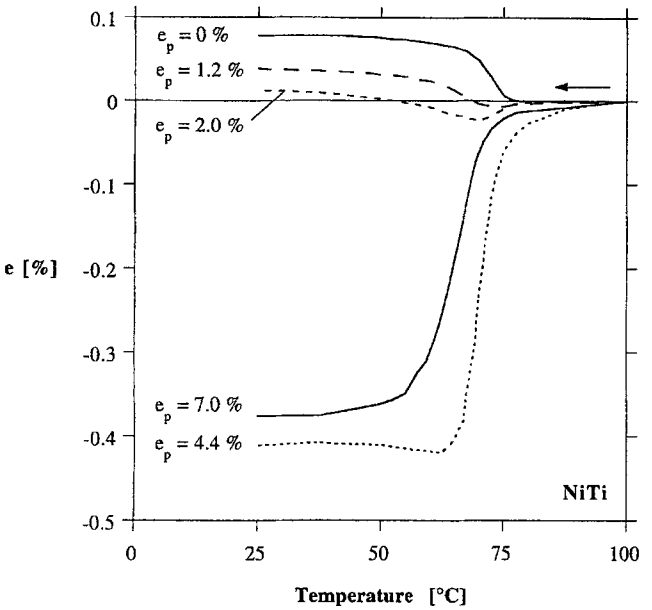

Fig. 9—Strain e upon cooling of NiTi deformed to different prestrains e_p.

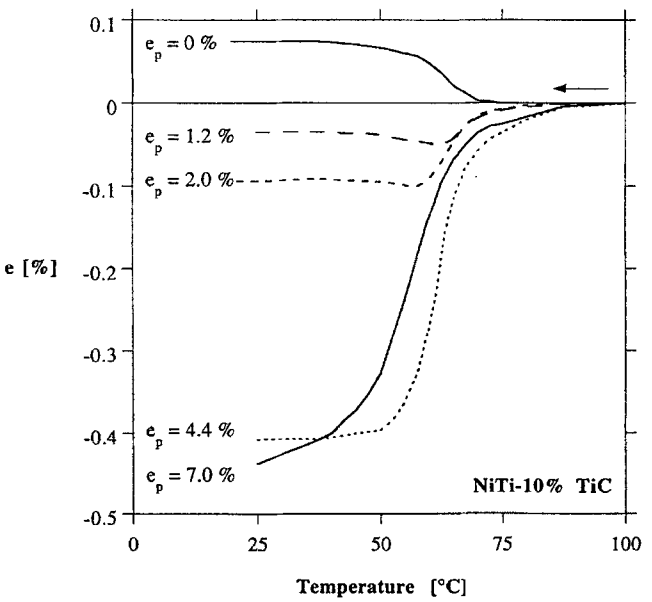

Fig. 10—Strain e upon cooling of NiTi-10TiC deformed to different prestrains e_p.

The volumetric transformation strain was calculated as $\Delta V/V = 1.6 \cdot 10^{-3}$ by Otsuka *et al.*[31] from lattice parameters determined by X-ray diffraction.[32] Direct measurements of the volume change for the ($\beta \rightarrow M$) transformation were performed by Hsu *et al.*,[30] who found volumetric expansions of $\Delta V/V = 1.9 \cdot 10^{-3}$ by hydrostatic weighing and $\Delta V/V = 2.2 \cdot 10^{-3}$ by multiaxial strain gage measurements. Assuming isotropic transformation strains, the corresponding linear allotropic expansion $\Delta L/L \approx (\Delta V/V)/3 = 6.3$ to $7.3 \cdot 10^{-4}$ is in reasonable agreement with our measurements by dilatometry for unreinforced NiTi ($\Delta L/L = 7.8 \cdot 10^{-4}$) and measurements by dilatometry for as-cast, stoichiometric NiTi ($\Delta L/L = 8 \cdot 10^{-4}$) reported in Reference 33.

Our as-processed NiTi specimens, consolidated by hot pressing of randomly oriented powders, can be considered

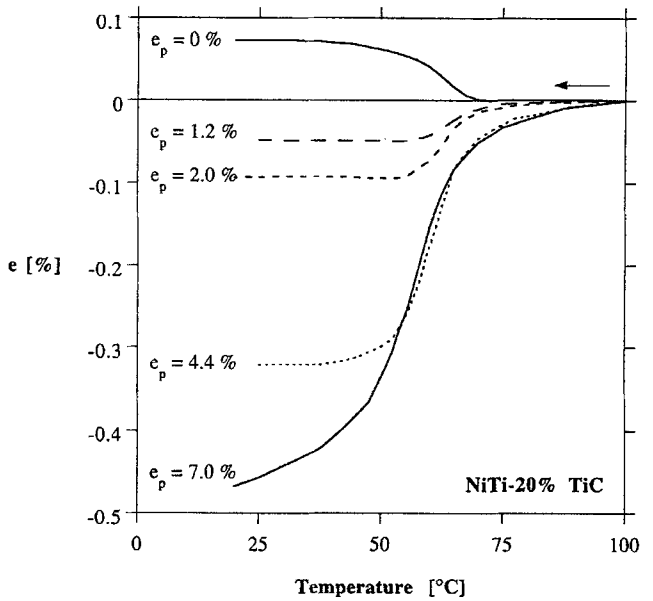

Fig. 11—Strain e upon cooling of NiTi-20TiC deformed to different prestrains e_p.

near isotropic. However, as shown in Figure 5, twinning texture resulting from strains as small as 2 pct significantly alters the recovery behavior of NiTi. Therefore, comparison with other literature values measured on anisotropic specimens produced by extrusion or cold drawing[13,34,35] is not attempted. Not only does the deformation texture lead to anisotropic length change,[30] but as discussed earlier, residual internal stresses can also induce the TWSME which reduces the recovery R measured at room temperature after the first thermal recovery cycle (Figures 9 and 16).

2. *NiTi-TiC Composites*

While the transformation temperatures measured by dilatometry and calorimetry are not directly comparable because the sensitivity of these methods is different, we note that most of the trends observed in Figures 8 and 12 (lower transformation temperatures and broader transformation temperature interval with increasing TiC content) have also been observed in our earlier calorimetry study of these undeformed materials.[22] The interpretation of the effect of TiC particulates on the transformation temperatures is complicated by the rhombohedral R phase,[22] the presence or absence of which is not detectable by dilatometry.

The coefficient of thermal expansion α_c of an isotropic composite containing spherical particles can be calculated with the Eshelby technique as[36]

$$\alpha_c = f_m\alpha_m + f_p\alpha_p + f_pf_m(\alpha_p - \alpha_m)\frac{K_p - K_m}{f_pK_p + f_mK_m + 3K_pK_m/(4G_m)} \quad [5]$$

where f is the volume fraction, K is the bulk modulus, G is the shear modulus, and the subscripts m, p, and c refer to the matrix, particles, and composite, respectively. As shown in Table I, the measured values for the composites are in agreement (within experimental error) with values calculated from Eq. [5], using the elastic constants for TiC given by Chang and Graham,[37] the average elastic constants calculated in the Appendix of Reference 24 from neutron diffraction and ultrasonic measurements for mar-

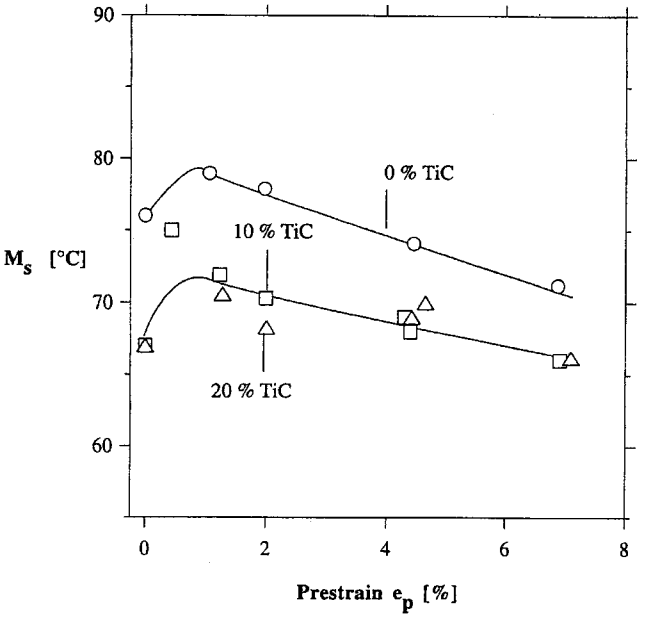

(*a*)

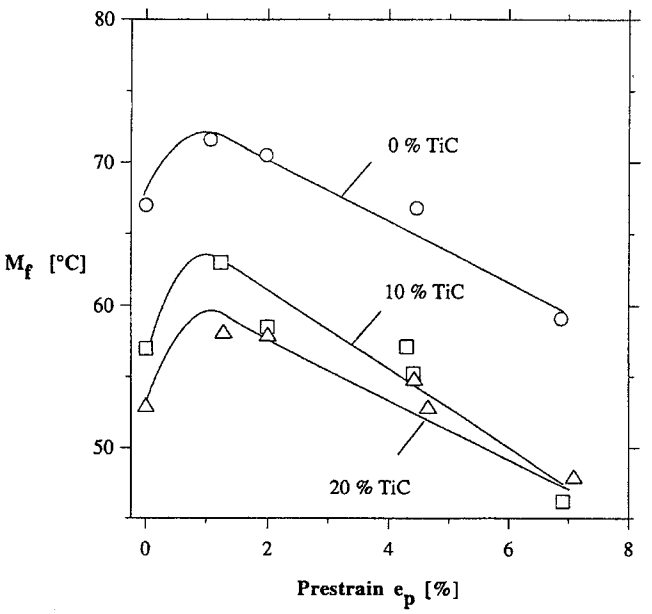

(*b*)

Fig. 12—(*a*) Martensite start temperature M_s and (*b*) Martensite finish temperature M_f (measured by dilatometry) as a function of prestrain e_p.

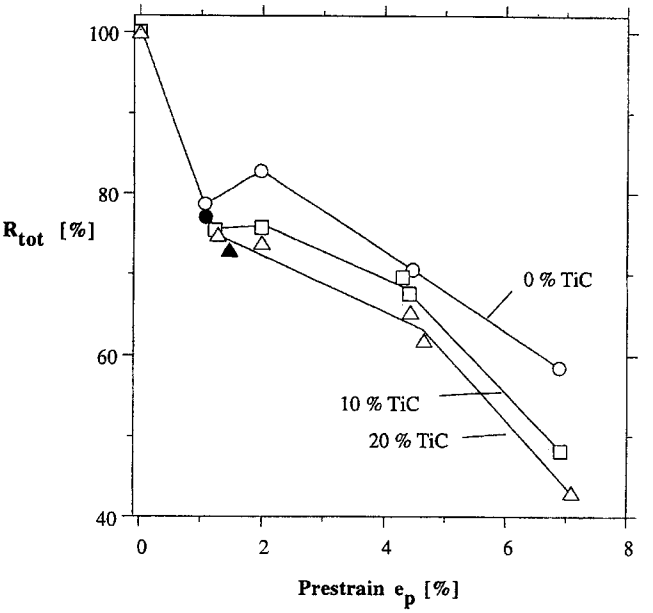

Fig. 13—Total extent of recovery after a full cycle, R_{tot}, as a function of prestrain e_p. Filled symbols correspond to data from a companion article.[24]

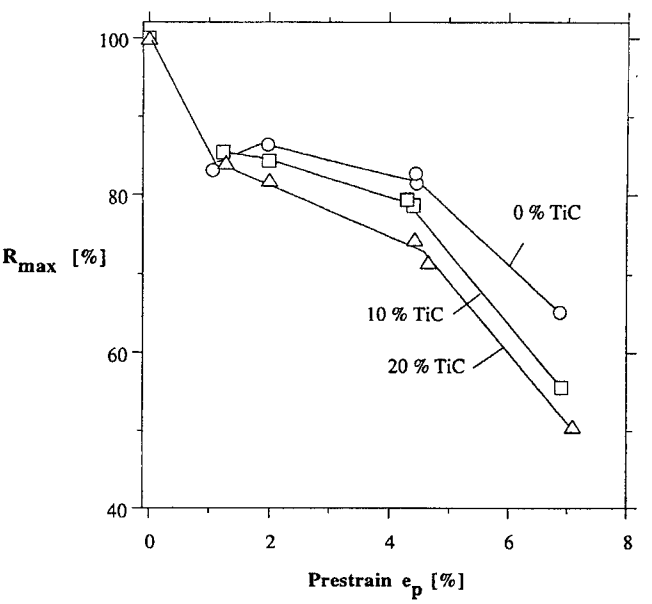

Fig. 14—Extent of recovery at the end of the heating cycle, R_{max}, as a function of prestrain e_p.

tensitic NiTi, and the thermal expansion coefficients given in Reference 38 for TiC and measured in the present work for unreinforced NiTi (Table I). The agreement between experimental and theoretical values indicates that thermal mismatch stresses in the matrix are not significantly relaxed by twinning (in the martensite) or formation of stress-induced martensite (in the austenite), since these mechanisms would alter the thermal expansion of the composite by inducing a twinning texture or by lowering the overall expansion coefficient, respectively.

In the following, we modify Eq. [5] to predict the length change occurring over the temperature $\Delta T = M_s - M_f$ due to the density change during the allotropic transformation. We set the linear allotropic expansion $\Delta L/L$ upon phase transformation equal to a fictitious thermal expansion over the temperature interval ΔT:

$$\left(\frac{\Delta L}{L}\right)_c = \alpha_c \Delta T \qquad [6a]$$

$$\left(\frac{\Delta L}{L}\right)_m = \alpha_m \Delta T \qquad [6b]$$

$$\left(\frac{\Delta L}{L}\right)_p = \alpha_p \Delta T = 0 \qquad [6c]$$

for the composite, matrix, and particles, respectively. Introduction of Eqs. [6a] through [6c] into Eq. [5] yields an equation for the linear allotropic expansion of the composite $(\Delta L/L)_c$:

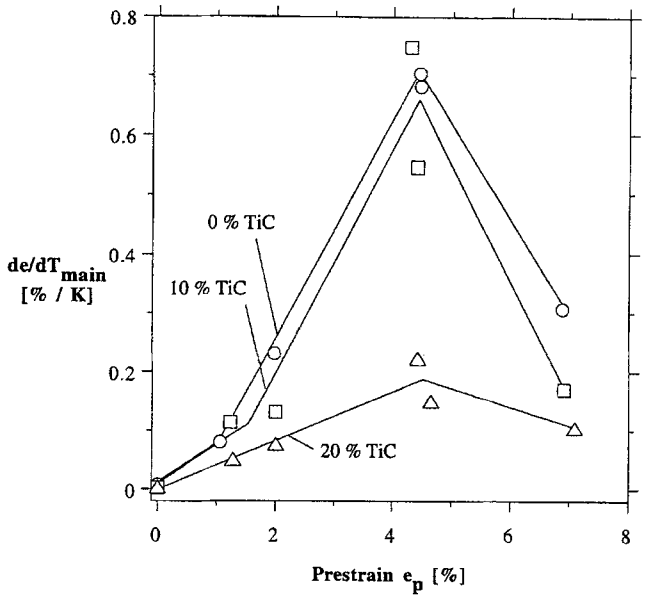

Fig. 15—Recovery strain gradient in region 2, de/dT_{main}, as a function of prestrain e_p.

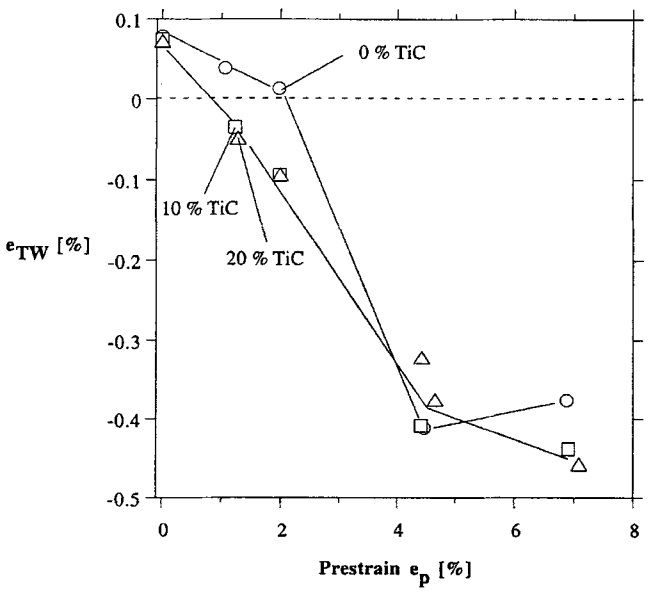

Fig. 16—Recovery strain in region 5, e_{TW}, as a function of prestrain e_p.

$$\left(\frac{\Delta L}{L}\right)_c = f_m \left(\frac{\Delta L}{L}\right)_m \left[1 - \frac{f_p (K_p - K_m)}{f_p K_p + f_m K_m + 3K_p K_m/(4G_m)}\right] \quad [7]$$

Table II lists for both composites the predictions from Eq. [7], taking the measured value $(\Delta L/L)_m = 7.81 \cdot 10^{-4}$ and the martensitic matrix parameters used for Eq. 5. Unlike the case of composite thermal expansion described previously where experimental results and predictions from Eq. [5] are in agreement, the measured linear allotropic expansion of the composites is larger than predicted by Eq. [7]. Varying the shear and compression moduli of the matrix by 50 pct does not significantly alter the calculated values, indicating that the modulus anomaly at the allotropic transformation temperature cannot explain the discrepancies. Experimental accuracy is not responsible either, as the displacement differences between measured and predicted values (0.6 μm for NiTi-10TiC and 1.3 μm for NiTi-20TiC) are higher than the measurement accuracy. We discuss in the following possible reasons for the preceding discrepancies.

In an earlier publication,[22] the transformation enthalpy of the matrix was found to decrease with increasing TiC content, as measured by calorimetry between −10 °C and 140 °C. This observation was explained by proposing that part of the matrix is stabilized and does not transform during the temperature cycle due to dislocations produced by the mismatch between particles and matrix. Since the expected effect, *i.e.*, reduction of the linear allotropic expansion $\Delta L/L$ for the composites as compared to the prediction of Eq. [7], is opposite to the observed trend (Table II), we cannot retain this explanation for the previous discrepancies.

The high values for the composite linear allotropic expansion can be explained if the mismatch from the transformation of the matrix in the presence of nontransforming particles is partially relaxed by twinning of the matrix. In the extreme case of a second phase exhibiting no mismatch during transformation (*i.e.*, if the second phase consists of pores with $K_p = 0$), Eq. [7] predicts that the linear allotropic expansion for the composite is the same as that of the matrix, as intuitively expected. The same result would be expected if the mismatch strains developed during the ($\beta \rightarrow M$) transformation are completely relaxed by the formation of twinned martensite in the vicinity of the particles, a mechanism similar to self-accommodation between variants in unreinforced NiTi. We note that twinning alone, which is a volume-conserving operation, cannot accommodate a purely isostatic mismatch. While the average matrix stress is hydrostatic after the transformation, as calculated in companion articles,[22,24] spatially resolved stress analysis indicates that the stress field in the matrix contains deviatoric components.[39] These deviatoric stresses can be partially relaxed by matrix twinning, resulting in a linear allotropic expansion of the composite larger than predicted by Eq. [7], for which no relaxation was assumed.

B. *Deformed Specimens*

1. *NiTi*

Mechanical prestrain in martensitic NiTi can be separated in three components: (1) plastic strain by twinning which is recoverable, (2) plastic strain by slip which is unrecoverable, and (3) residual elastic strains, which do not on average contribute to the total macroscopic prestrain but may be recovered by relaxation during phase transformation. These three types of strains affect the kinetics and thermodynamics of the transformation as follows: (1) twinning reduces the number of martensitic variants, thus facilitating their subsequent transformation to austenite, and may also induce residual elastic stresses due to mismatch strains between twinned variants; (2) dislocations introduced by slip both stabilize the deformed martensite and induce the TWSME by their elastic stress field, as described earlier; and (3) elastic stresses stabilize the martensite, as described by the Clausius–Clapeyron equation, and can induce the TWSME. Based on these three effects, the features of the NiTi dilatometric curves are discussed in the following.

Figure 13 shows that the magnitude of the recovery R

after a complete thermal cycle is significantly less than 100 pct for unreinforced NiTi. Incomplete recovery of about 50 pct was also reported by Johnson *et al.*[40] for NiTi samples fabricated by powder metallurgy after tensile prestrains of 2 to 10 pct. On the other hand, Reference 13 reported complete strain recovery for cast and hot-worked NiTi rods deformed to tensile prestrains of 6 to 8 pct and compressive prestrains of about 4 pct. Wasilewski[41] measured a recovery of 94 pct upon heating in the austenitic phase for stoichiometric NiTi deformed to a prestrain of 4.3 pct but significantly less net recovery after subsequent cooling to room temperature because of a large TWSME.

The lack of complete recovery after a complete cycle in our NiTi samples, however, is not due to the TWSME, because, as shown in Figure 14, the recovery in the austenite at the maximum temperature of 275 °C is at most about 85 pct. Another interpretation for the incomplete recovery is that the twinned martensite is not fully transformed because the structure is stabilized by dislocations. While the positive slope de/dT_{post} of the postrecovery region 3 of all dilatometric curves (Figure 4) indicates that some transformation is indeed taking place at temperatures as high as 275 °C, the fraction of M' transformed in region 3 is very small (a few percent for the highest prestrain e_p = 7 pct, Figure 5). However, it seems unlikely that large amounts of stabilized martensite exist at a temperature more than 130 K above A_f. Finally, we note that residual internal stresses after deformation are likely to be small on average because of self-accommodation by twinning during loading and unloading. This was verified by neutron diffraction measurements of NiTi samples deformed in compression to a prestrain e_p = 1.6 pct, which indicated negligible average residual stresses.[24]

It thus appears that upon compressive deformation of NiTi samples, substantial unrecoverable deformation by slip occurs concurrently with recoverable deformation by twinning, even for prestrains as low as 1.2 pct. Assuming that the unrecoverable strain (Figure 14) is equal to the plastic deformation by slip, the latter represents about 15 pct of the total plastic strain for prestrain values e_p between 1 and 4.4 pct, *i.e.*, in a regime where twinning is expected to be the dominant deformation mechanism (Figure 2). For a prestrain e_p = 7 pct, where generalized slip occurs (Figure 2), the extent of recovery further decreases by about ΔR = 20 pct to a value of about 65 pct (Figure 14). The corresponding irrecoverable strain is $\Delta R \cdot e_p$ = 1.40 pct, a value close to the plastic strain by slip of about 1.45 pct measured on the stress-strain curve (Figure 2) as the offset from the "elastic" loading line spanning the linear M' stress region between 600 and 1000 MPa.

Further indications of slip deformation for all prestrains are the monotonic increase of the transformation temperatures A_s and A_f (Figures 8(a) and (b)) and the monotonic decrease of the temperatures M_s and M_f (Figures 12(a) and (b)) with increasing prestrain. The increasing transformation hysteresis resulting from these trends can be explained by dislocations which oppose the transformation by exerting a friction stress on the moving interface during transformation and which therefore increase the undercooling and overheating required beyond the equilibrium chemical transformation temperature. We note that similar trends have been reported by Johnson *et al.*[40] for NiTi deformed in tension, except for the weak increase of M_s with increasing prestrain reported by these authors.

As depicted in Figure 15, the main recovery gradient de/dT_{main} in region 2 of the dilatometric curve increases linearly with prestrain up to e_p = 4.4 pct, above which it decreases abruptly. The initial increase of de/dT_{main} can be explained as follows: with increasing prestrain, the number of variants decreases because of twinning, so the range of transformation temperature A_f to A_s is narrowed (a single crystal would transform at a single temperature). The decrease of de/dT_{main} for e_p = 7 pct can be explained by slip deformation at high strains (Figure 2). It is probable that some variants undergo more slip (and are thus more stabilized) than others, therefore, widening the transformation temperature interval. Furthermore, elastic residual stresses, which increase with prestrain, have the same widening effect, because they increase the average transformation temperatures upon heating (Clausius–Clapeyron equation). Finally, the development of an inhomogenous distribution of elastic and plastic strains can also explain the increased strain recovered in the pre- and postrecovery regions 1 and 3 observed with increasing prestrain in Figure 5.

Upon transformation during cooling in region 5, the TWSME occurs abruptly for prestrains above 2 pct (Figures 9 and 16), corresponding to samples exhibiting large-scale plastic deformation by slip (Figure 2). This is in agreement with reports that training for TWSME necessitates plastic deformation by slip of the martensite.[4,10,42] However, the value of the TWSME strain e_{TW} = 0.4 pct at the maximum prestrain e_p = 4.4 pct is significantly smaller than the value e_{TW} = 1.5 pct reported by Wasilewski[41] for stoichiometric NiTi deformed in compression at 0 °C to a similar prestrain e_p = 4.3 pct.

A small TWSME is present for prestrains less than 2 pct: the dilatometric curves in Figure 9 show that the transformation starts with an expansion (TWSME) and finishes with a contraction (SME). This behavior may be the result of inhomogenous deformation by slip: some variants were deformed by slip, resulting in the initial TWSME, while other variants were deformed by twinning, leading to the subsequent SME. This is in agreement with the observations made previously that plastic deformation by slip is responsible for about 15 pct of the deformation of the composites, as shown by the incomplete extent of recovery upon heating (Figure 14) and as also reported in an earlier article.[23]

2. *NiTi-TiC Composites*

The presence of a nontwinning second phase within a twinning NiTi matrix may affect the mechanical deformation and the subsequent thermal recovery of the matrix in different ways, depending on the deformation behavior of the particulate second phase. If the particles are plastically deformed by slip during mechanical prestrain, and if their yield stress is less than the critical stress for twinning of the matrix, they induce no plastic mismatch in the matrix during mechanical deformation. However, if the particles exhibit a yield stress which is higher than the critical twinning stress of the matrix but lower than the maximum stress experienced by the composite during prestrain, they produce an elastic mismatch before deforming plastically by slip, which may alter the matrix microstructure and the level of residual elastic stresses. In both cases, the particles

exert a back stress by opposing the transformation upon subsequent thermal recovery, thus expanding the transformation temperature hysteresis and reducing the recovery R, as demonstrated by Duerig co-workers[43,44] for NiTi containing a plastically deforming niobium-rich second phase.

The mismatch between a twinning NiTi matrix and stiff, elastic reinforcing particles such as TiC cannot be relaxed by the reinforcement, provided it does not fracture in the bulk or at the interface. However, relaxation of the elastic and plastic mismatches between the two phases may occur by twinning or slip of the matrix. In the first case, transformation upon heating of mismatch twins formed during mechanical deformation to accommodate the elastic particles is similar to transformation of twins responsible for the overall shape change of the specimen. Thus, the overall recovery behavior of the composite is expected to show little difference with that of the unreinforced matrix. In the second case, where matrix slip from mechanical deformation relaxed the mismatch with the reinforcement, dislocations are expected to stabilize the deformed martensite and enhance the TWSME, as observed in unreinforced NiTi deformed by slip. Furthermore, if relaxation by slip or twinning is incomplete after deformation, the resulting residual elastic stresses are expected to affect the macroscopic recovery behavior by stabilizing the martensite and by inducing the TWSME. Residual elastic stresses after deformation, however, are expected to be small on average: as measured by neutron diffraction,[24] average residual elastic stresses in NiTi-20TiC were negligible after unloading from a prestrain $e_p = 2$ pct, because the matrix accommodated the mismatch by localized twinning.

Of the three types of residual strains (twinning, slip, and elastic) resulting from the plastic mismatch between the TiC particles and the NiTi matrix, only the latter two are expected to influence the recovery behavior of the deformed composites, as discussed previously. First, increased slip deformation of the matrix can explain the following observations.

(1) The extent of recovery R_{max} decreases with increasing TiC content for prestrains larger than $e_p = 1.4$ pct (Figure 14). This indicates that unrecoverable deformation by slip increases in the composites.
(2) With increasing TiC fractions, the strain recovery during the pre- and post-transformation (regions 1 and 3, Figure 3) increases and the recovery gradient de/dT_{main} during the main recovery in region 2 (Figure 3) decreases, as shown in Figure 15. These two phenomena broaden the recovery temperature interval, as expected if the martensitic variants close to the particles contain more mismatch dislocations (and are thus more stabilized) than the variants far from the particles.
(3) The magnitude of the TWSME strain increases with increasing TiC content (Figure 16), as expected if the composites contain more dislocations, the elastic stress field of which biases the formation of oriented martensite.

We note that plastic deformation in the composites due to the presence of TiC particles reduces the total extent of recovery after a full cycle R_{tot} (Figure 13) both by decreasing the magnitude of the recoverable plastic strain by slip (effect (1), Figure 14) and by increasing the magnitude of the TWSME strain (effect (3), Figure 16).

Second, residual elastic strains in the composites can explain the following observations.

(4) The transformation temperatures A_s, A_f, M_s, and M_f all decrease with increasing TiC content (Figures 8 and 12), in agreement with the effect of elastic stresses on a thermoelastic transformation.[45]
(5) The magnitude of the TWSME strain increases with increasing TiC content (Figure 16). While this effect can be explained by plastic deformation (item (3) earlier), elastic stresses due to incomplete relaxation in the composite can also have the same effect.

We thus conclude that the systematic trends observed in the recovery curves of the composites can be explained by an increase in plastic strains in the matrix and increased residual elastic stresses due to the mismatch between the matrix and the reinforcement during compressive deformation. In most cases, however, the difference in recovery properties between reinforced and unreinforced NiTi is relatively minor, indicating that most of the mismatch is accommodated by twinning. These conclusions reinforce similar conclusions reached in an earlier article[23] based on the shape of the stress-strain curves of NiTi-TiC composites and those in a companion paper[24] based on neutron diffraction measurements of internal strains during and after deformation.

V. CONCLUSIONS

The shape-memory recovery behavior of NiTi was investigated as a function of compressive mechanical prestrain and compared to that of NiTi composites containing 10 and 20 vol pct particulates. The following points summarize the main findings of this study.

1. For undeformed, unreinforced NiTi specimens, the linear allotropic expansion for the ($\beta \rightarrow M$) transformation is $\Delta L/L = 7.8 \cdot 10^{-4}$, in reasonable agreement with hydrostatic weighting measurements reported by Hsu *et al.*[30] The coefficients of thermal expansion for martensitic and austenitic NiTi are, respectively, $\alpha_M = 8.5 \cdot 10^{-6}\ K^{-1}$ and $\alpha_A = 12.1 \cdot 10^{-6}\ K^{-1}$, in good agreement with literature values.
2. Undeformed NiTi-TiC composites exhibit linear allotropic expansion and linear thermal expansion coefficients smaller than those of undeformed, unreinforced NiTi. The thermal expansion values are in agreement with predictions from a continuum mechanics equation assuming no relaxation of the thermal mismatch between the two phases. A simple equation is developed for the linear allotropic expansion of a composite. The observed expansion is larger than predicted by this equation, indicating that transformation mismatch elastic strains are partially accommodated by twinning of the matrix.
3. In deformed, unreinforced NiTi, substantial plastic deformation by slip for mechanical prestrains between 1.2 and 4.4 pct (for which twinning is expected to be the main deformation mechanism) is responsible for the following trends in the recovery behavior as the prestrain

increases: (a) an incomplete shape recovery of about 85 pct, (b) an increase of the transformation hysteresis, (c) an increase in the temperature span over which recovery occurs, and (d) an increase in the TWSME. For prestrains of 7 pct, where large-scale plastic deformation by slip occurs, these trends are also observed.

4. In deformed NiTi-TiC composites, the mismatch between the elastic TiC particles and the NiTi matrix must be relaxed by additional matrix plastic strain: unrecoverable slip deformation or recoverable twinning. Both the SME and the TWSME are affected little by the presence of up to 20 vol of ceramic particles, indicating that a major part of the mismatch is relaxed by matrix twinning. The thermal recovery behavior of the composites indicates that plastic strain by slip increases as the TiC content increases: the magnitude of recoverable strain decreases, the transformation is spread over a wider temperature range, and the TWSME is enhanced. The last effect and the decrease of all transformation temperatures can also be explained by the enhanced residual elastic stresses in the composites.

ACKNOWLEDGMENTS

This research was supported, in part, by the National Science Foundation Materials Research Laboratory (Grant No. DMR90-22933), administered through the Center for Materials Science and Engineering at MIT. DCD acknowledges the support of AMAX, in the form of an endowed chair at MIT. The authors are thankful to Dr. D. Mari (Advanced Composite Materials Engineering) for helpful discussions and to Professor T.W. Eagar (MIT) for use of experimental facilities.

REFERENCES

1. C.M. Wayman: *Met. Forum*, 1981, vol. 4, pp. 135-41.
2. J. Perkins: *Met. Forum*, 1981, vol. 4, pp. 153-63.
3. T. Saburi and S. Nenno: in *Solid-Solid Phase Transformations*, H.I. Aaronson, D.E. Laughlin, R.F. Sekerka, and C.M. Wayman, eds., TMS-AIME, Warrendale, PA, 1982, pp. 1455-79.
4. K. Otsuka and K. Shimizu: *Int. Mater. Rev.*, 1986, vol. 31, pp. 93-114.
5. K. Shimizu and T. Tadaki: in *Shape Memory Alloys*, H. Funakubo, ed., Gordon and Breach, New York, NY, 1987, pp. 1-60.
6. T. Honma: in *Shape Memory Alloys*, H. Funakubo, ed., Gordon and Breach, New York, NY, 1987, pp. 61-115.
7. C.M. Wayman and J.D. Harrison: *J. Met.*, 1989, vol. 41, pp. 26-28.
8. C.M. Friend: *J. Phys. IV*, 1991, vol. 1, pp. C4-25-C4-34.
9. E. Hornbogen: in *Progress in Shape Memory Alloys*, S. Euken, ed., DGM, Oberursel, Germany, 1992, pp. 3-19.
10. C.M. Wayman: *MRS Bull.*, 1993, vol. 18, pp. 49-56.
11. T.W. Duerig and A.R. Pelton: *Materials Properties Handbook: Titanium Alloys*, R. Boyer, G. Welsch, and E.W. Collings, eds., ASM INTERNATIONAL, Materials Park, OH, 1994, pp. 1035-48.
12. L.M. Schetky: *Robotics Age*, 1984, pp. 13-17.
13. C.M. Jackson, H.J. Wagner, and R.J. Wasilewski: NASA-SP 5110, 1972, pp. 23-88.
14. E. Hornbogen: in *Advanced Structural and Functional Materials*, W.G.J. Bunk, ed., Springer-Verlag, New York, NY, 1991, pp. 133-63.
15. T. Stevens: *Mater. Eng.*, 1991, vol. 108, pp. 18-20.
16. Y. Suzuki and Y. Sekiguchi: *Shape Memory Alloys*, H. Funakubo, ed., Gordon and Breach, New York, NY, 1987, pp. 176-269.
17. D. Stoeckel: *Adv. Mater. Proc.*, 1990, vol. 138 (10), pp. 33-36.
18. R.G. Gilbertson: *Muscle Wires Project Book*, Mondo-tronics, San Anselmo, CA, 1994, pp. 1-22.
19. K. Escher and E. Hornbogen: *J. Phys. IV*, 1991, vol. 1, pp. C4-427-C4-432.
20. E. Hornbogen, M. Thumann, and B. Velten: in *Progress in Shape Memory Alloys*, S. Eucken ed., DGM, Oberursel, Germany, 1992, pp. 225-36.
21. L.C. Zhao, T.W. Duerig, S. Justi, K.N. Melton, J.L. Proft, W. Yu, and C.M. Wayman: *Scripta Metall. Mater.*, 1990, vol. 24, pp. 221-226.
22. D. Mari and D.C. Dunand: *Metall. Mater. Trans. A*, 1996, vol. 26A, pp. 2833-48.
23. K.L. Fukami-Ushiro, D. Mari, and D.C. Dunand: *Metall. Mater. Trans. A*, 1996, vol. 27A, pp. 183-191.
24. D.C. Dunand, D. Mari, M.A.M. Bourke, and J.A. Goldstone: *Metall. Mater. Trans. A.*, in press.
25. K.L. Fukami: Master's Thesis, Massachusetts Institute of Technology, Cambridge, MA, 1994.
26. *Smithells Metals Reference Book*, E.A. Brandes and G.B. Brook, eds., Butterworth-Heinemann, Oxford, United Kingdom, 1992, p. 27.5.
27. *Metals Handbook: Properties and Selection: Nonferrous Alloys and Pure Metals*, ASM, Metals Park, OH, 1979, p. 64.
28. W.A. Backofen: *Deformation Processing*, Addison-Wesley, Reading MA, 1972, pp. 162-68.
29. T.E. Buchheit and J.A. Wert: *Metall. Mater. Trans. A*, 1994, vol. 25A, pp. 2383-89.
30. C.H. Hsu, M.S. Wechsler, and H. Diehl: Ames Laboratory Report No. IS-4799, Ames, IA, 1982, pp. 1-19.
31. K. Otsuka, T. Sawamura, K. Shimizu, and C.M. Wayman: *Metall. Trans.*, 1971, vol. 2, pp. 2583-88.
32. K. Otsuka, T. Sawamura, and K. Shimizu: *Phys. Status Solidi*, 1971, vol. 5, pp. 457-70.
33. I.I. Kornilov, Y.V. Kachur, and O.K. Belousov: *Fiz. Met. Metalloved.*, 1971, vol. 32, pp. 420-22.
34. C.H. Hsu and M.S. Wechsler: in *Solid-Solid Phase Transformations*, H.I. Aaronson, D.E. Laughlin, R.F. Sekerka, and C.M. Wayman, eds., TMS-AIME, Warrendale, PA, 1982, pp. 1293-97.
35. H.C. Ling and R. Kaplow: *Mater. Sci. Eng.*, 1981, vol. 51, pp. 193-201.
36. M. Taya and R.J. Arsenault: *Metal Matrix Composites—Thermomechanical Behavior*, Pergamon Press, Oxford, United Kingdom, 1989, pp. 177-208.
37. R. Chang and L.J. Graham: *J. Appl. Phys.*, 1966, vol. 37, pp. 3778-83.
38. *The CRC Materials Science and Engineering Handbook*, J. Shackelford and W. Alexander, eds., CRC Press, Boca Raton, FL, 1992, p. 358.
39. E. Sato and K. Kuribayashi: *Acta Metall. Mater.*, 1993, vol. 41, pp. 1759-67.
40. W.A. Johnson, J.A. Domingue, S.H. Reichman, and F.E. Sczerzenie: *J. Phys.*, 1982, vol. 43, pp. C4-291-C4-296.
41. R.J. Wasilewski: *Scripta Metall.*, 1975, vol. 9, pp. 417-22.
42. G. Guenin: *Phase Transitions*, 1989, vol. 14, pp. 165-75.
43. T.W. Duerig and K.N. Melton: *The Martensitic Transformation in Science and Technology*, E. Hornbogen and N. Jost, eds., DGM, Oberursel, Germany, 1989, pp. 191-98.
44. L.C. Zhao, T.W. Duerig, S. Justi, K.N. Melton, J.L. Proft, W. Yu, and C.M. Wayman: *Scripta Metall. Mater.*, 1990, vol. 24, pp. 221-26.
45. R.J. Salzbrenner and M. Cohen: *Acta Metall.*, 1979, vol. 27, pp. 739-48.